

# Novel poly(aryl ether ketone) with electro-optic chromophore side chains for light modulators

Jian Zhou<sup>1</sup> · Jialei Liu<sup>2</sup> · Min Wang<sup>1</sup> · Wenjun Hou<sup>2</sup> · Guangjiong Qin<sup>6</sup> · I. V. Kityk<sup>3</sup> · A. A. Fedorchuk<sup>8</sup> · A. A. Albassam<sup>4</sup> · A. M. El-Naggar<sup>4,5</sup> · A. Andrushchak<sup>7</sup>

Received: 16 August 2017 / Accepted: 28 August 2017 / Published online: 4 September 2017  
© The Author(s) 2017. This article is an open access publication

**Abstract** Organic nonlinear optical materials have been widely explored because of their advantages in the design of materials with large electro-optic coefficients used in the fabrication of novel optoelectronic and telecommunication devices. However, the huge dipole–dipole interactions between organic nonlinear optical chromophores have limited further improvements in the electro-optic coefficients and long-term material stability. Here, a novel polymer based on poly(aryl ether ketone) was designed and prepared to enhance the electro-optic coefficients and achieve higher long-term stability. This novel poly(aryl ether ketone) has a relatively high glass transition temperature and offers active functional groups for the attachment of organic nonlinear optical chromophores. After attachment of nonlinear optical chromophores the materials showed higher chromophore loading density, less inter-molecular interaction, and suitable solubility. This resulted in better film-forming ability, higher electro-optics coefficients and better long-term stability. Quantum chemical simulations of the second order

hyperpolarizabilities and ground state dipole moments were done to understand the origin of the effects.

## 1 Introduction

Due to their ultrafast response time, easier processing, lower dielectric constant and higher nonlinear optical coefficients compared to conventional inorganic crystals and semiconductors, organic second order nonlinear optical materials have received more and more attention for their potential applications in high speed electro-optic conversion devices [1–7]. The performance of electro optical (EO) devices in half-wave voltage, insertion loss and stability has increased. Thus, the performance of organic nonlinear optical materials should also be improved for electro optic coefficients, thermal stability, photochemical stability, long-term stability and optical loss [8–12]. Though many organic second order nonlinear optical chromophores exhibiting large macroscopic nonlinear optical coefficients in poled guest–host

✉ I. V. Kityk  
iwank74@gmail.com; liujialei@mail.ipc.ac.cn

<sup>1</sup> Institute of Quality Standards and Testing Technology for Agro-Products/Key Laboratory of Agro-Product Quality and Safety, Chinese Academy of Agriculture Sciences, Beijing 100081, People's Republic of China

<sup>2</sup> Key Laboratory of Photochemical Conversion and Optoelectronic Materials, Technical Institute of Physics and Chemistry, Chinese Academy of Sciences, Beijing 100190, People's Republic of China

<sup>3</sup> Faculty of Electrical Engineering, Institute of Optoelectronics and Measuring Systems, Czestochowa University Technology, Armii Krajowej 17, 42201 Czestochowa, Poland

<sup>4</sup> Research Chair of Exploitation of Renewable Energy Applications in Saudi Arabia, Physics and Astronomy Department, College of Science, King Saud University, P.O. Box 2455, Riyadh 11451, Saudi Arabia

<sup>5</sup> Physics Department, Faculty of Science, Ain Shams University, Abasia, Cairo 11566, Egypt

<sup>6</sup> Tobacco Research Institute of Hubei Province, Wuhan 430030, China

<sup>7</sup> Lviv Polytechnic National University, 12 Bandera Str., Lviv 79013, Ukraine

<sup>8</sup> Faculty of Chemistry, Ivan Franko National University of Lviv, Lviv, Ukraine

polymers have been reported in the past two decades, it is very difficult to find organic second order nonlinear optical materials that have both large electro optic coefficients and long-term stability [13–18]. Due to the large EO coefficients of about 42–78 pm/V (all the EO parameters are given at wavelength 1.3  $\mu\text{m}$ ) at low chromophore loading density (10 wt%), chromophore CLDs have been widely studied, but their thermal decomposition temperature is very low ( $\sim 180^\circ\text{C}$ ) [53].

To solve this problem, researchers have focused on either the preparation of novel host polymers containing nonlinear optical chromophores in the main chains with high glass transition temperatures or they have introduced cross linking groups into the electro optic polymer systems [19–24]. Else, some advanced material structures (binary system) and poling or devices preparing technologies (slot electrode structure) were added to organic EO materials. Due to these advanced structures and technologies, the EO coefficients have been improved significantly (up to 300 pm/V) in the recent years [25–60].

Long-term stability could be improved in both systems. However, many new problems have emerged. In the first system, the nonlinear optical chromophores are hard to align, and the solubility is usually very poor [25, 26]. For the second system, the design of cross linkable groups is very difficult. Both of the cross linking conditions and the chemical stability of the chromophores in the cross linking process should be considered [27–30]. Fortunately, a compromised method was proposed: nonlinear optical chromophores were attached to the polymers with high glass transition temperatures as the side chain [31, 32]. This system demonstrates many advantages in solubility, homogeneity and loading density of nonlinear optical chromophores.

Two major approaches have been applied to the synthesis of side-chain nonlinear optical polymers. The first one is that the chromophore was functionalized with suitable groups to give a monomer. This is critical for the chromophores to bear the harsh conditions during polymerization, but it limits the selection of the chromophores. The second approach is to covalently connect the chromophore to the pendant side chain of the polymer, which we call post-functionalization. The advantage of post-functionalization is that different types of chromophores can be introduced into the polymer backbone [33–37].

Novel EO chromophores were predicted based on the optimization of a planar  $\pi$ -conjugation bridge and donor–acceptor moieties [54]. Most of the following approaches focus on prevalently intra-molecular charge transfer. The latter is a transition of electrons from ground state to excited state and creation of principal medium polarization. Here very popular is oversimplified two-state approach that can be presented as:

$$\beta = \frac{(\mu_{ee} - \mu_{gg})(\mu_{ge})^2}{(\Delta E_{ge})^2} \quad (1)$$

where  $\mu_{ee}$  and  $\mu_{gg}$  are the excited and ground state dipole moments, respectively;  $\mu_{ge}$  is the transition dipole moment between the ground and excited states; and  $\Delta E_{ge}$  is the energy interval between the ground and excited states.

Following the Eq. (1), one can see that the main efforts to enhance the corresponding nonlinear optical properties should be devoted to the charge space separated contribution through the following ways: (1) improving the electron withdrawing ability of the acceptor groups and the electron donating ability of the electron donor groups; (2) introduction of auxiliary donors or acceptors; and (3) extension of the electronic bridge.

Poly(aryl ether ketone) combines polymers with a linear chain composed of alternating aromatic rings and ketones or ether groups. This coexistence offers a good thermal stability, chemical stability, and mechanical properties. The shape and glass transition temperature should be considered with respect to the application of nonlinear optical materials. By adjusting the ratio of different monomers, such a polymers could exhibit an amorphous or semi crystalline form with respect to the known polymer chromophores. A higher glass transition temperature could be reached at higher contents of ketone linkages due to more rigid ketone structure. This property is convenient for us to adjust the glass transition temperature.

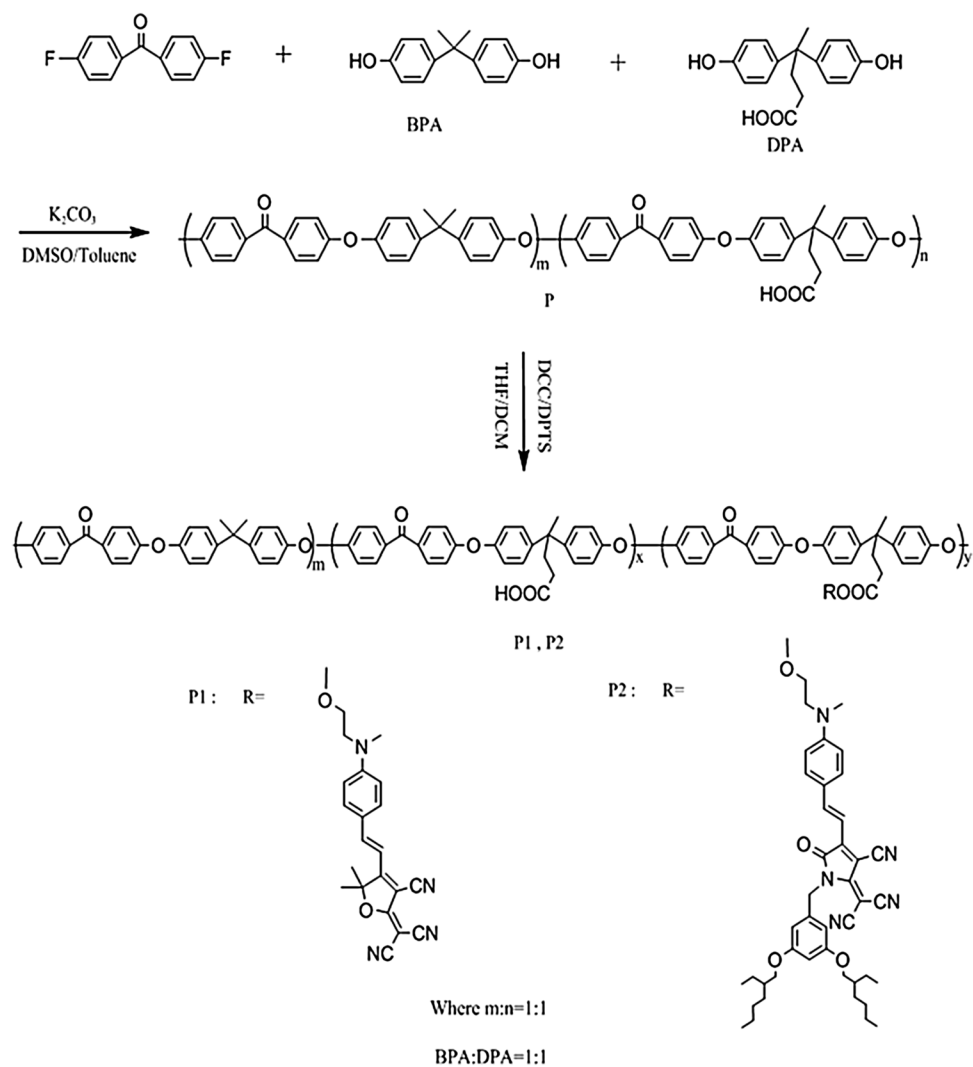
In this paper, bisphenol A, 4,4-bis(4-hydroxyphenyl) pentanoic acid and 4,4'-difluorobenzophenone are used as monomers. The carboxyl group in 4,4-bis(4-hydroxyphenyl) pentanoic acid can be applied to attach nonlinear optical chromophores. Polymers with a glass transition temperature of  $158^\circ\text{C}$  were chosen for the fabrication of electro-optics polymers because they have higher thermal stability of nonlinear optical chromophores. Chromophores with different electron acceptors and modified groups are also designed and prepared. The chromophores were attached to the polymer by post functional technology, which ensured that the chromophores were efficient. The thermal stability, electro-optics activity, solubility and long-term stability of the electro optic polymers will be presented below. It is necessary to add that these chromophore are also promising for the optical second harmonic generation.

## 2 Results and discussion

### 2.1 Synthesis of chromophore TCF-G and TCP-G

The structure of chromophores **TCF-G** and **TCP-G** are shown in Fig. 1. Chromophore **TCF-G** is formed by the

**Fig. 1** The synthesis process and molecular structure of EO polymer **P1** and **P2**



*N*-(2-hydroxyethyl)-*N*-methylaniline electronic donor, the 2-(3-cyano-4,5,5-trimethyl-5H-furan-2-ylidene)-malononitrile electronic acceptor and the carbon–carbon double bond electronic bridge. The donor- $\pi$ -acceptor structure confirms the non-centrosymmetric structure of this chromophore. Chromophore **TCP-G** was formed by an *N*-(2-hydroxyethyl)-*N*-methylaniline electronic donor, a 2-(3-cyano-4-methyl-5-oxo-1,5-dihydro-pyrrol-2-ylidene)-malononitrile electronic acceptor, a carbon–carbon double bond electronic bridge and a 3,5-bis-(2-ethyl-hexyloxy) benzyl-modified group. The large modified group confirmed the sufficient distance between the chromophores and improved the solubility of the chromophore. The synthesis of chromophore **TCF-G** and **TCP-G** has been reported in our earlier papers [28, 38]. They are both synthesized by a Knoevenagel condensation reaction [17, 19].

## 2.2 Synthesis of EO polymer **P1** and **P2**

The structure of the EO polymer **P1** and **P2** are shown in Fig. 1. A novel poly(aryl ether ketone) polymer was post-functionalized using organic second order nonlinear optical chromophore **TCF-G** and **TCP-G**. Compared with the common used polymethylmethacrylate (PMMA) host polymer, the rigid structure of polymer **P** confirmed the regularity of the polymer segments and high glass transition temperature, which favors the high poling ability and good long term stability. Compared with the common used polycarbonate (PC) host polymer, the ether linkage of polymer **P** performed stronger chemical stability than ester linkage in PC. This property afforded a positive role in the process of post-functionalization. Else, the electron donating ability of ether bond and electron withdrawing ability of ketone bond in the main chain afforded the host polymer of **P** with electron noncentrosymmetric structure. Though the first-order hyperpolarizability of polymer **P** is not too strong, it can

help us to improve the poling efficiency and long term stability by the inter-molecular inducing interaction.

Bisphenol A, 4,4-bis(4-hydroxyphenyl) pentanoic acid and 4,4'-difluorobenzophenone were used as the monomers. Aliphatic nucleophilic substitution was used in the preparation process. The reaction process is similar to the preparation process of normal poly aryl ether: (1) bisphenol A or 4,4-bis(4-hydroxyphenyl) pentanoic acid monomer reacted with potassium carbonate affording us negative oxygen ion; (2) negative oxygen ion was used as a nucleophilic reagent and reacted with 4,4'-difluorobenzophenone affording the Meisenheimer complex compound; and (3) the fluorine atom was reduced, the aliphatic nucleophilic substitution process was finished and the backbone polymer was fabricated. In this reactive process, the formation of Meisenheimer complex compound was rate-determining step due to the high energy level of the complex compound.

The 4,4-bis(4-hydroxyphenyl) pentanoic acid was a specific and principal monomer: (1) the phenolic hydroxyl groups could react with 4,4'-difluorobenzophenone affording us the backbone of the polymers; (2) the carboxyl group reacted with many groups that helped us to introduce the functional small molecules to the backbone of the polymers as a side chain. The reaction between the carboxyl group and hydroxyl group-affording ester is widely used in the post functionalization of polymers. In this paper, *N,N'*-dicyclohexylcarbodiimide (DCC) and 1,4-dimethylpyridinium *p*-toluenesulfonate (DPTS) were used as the dehydrating agent and the catalyst, respectively. Due to the mild reactive conditions (ambient temperature), weak alkalinity and high yield, this esterification process was suitable for the preparation of side chain nonlinear optical polymers.

All chemicals are commercially available and used without further purification unless otherwise stated. Chromophore TCF-G and TCP-G were prepared according to the literature [43]. <sup>1</sup>H-NMR spectra were measured by an Advance Bruker 400M (400 MHz) NMR spectrometer (tetramethylsilane as internal reference). The FT-IR spectra were determined by Bruker Tensor spectrometer. The UV-Vis experiments were performed on Cary 5000 spectrophotometer with spectral resolution 1 nm. The glass transition temperature was determined by Q20DSC (TA co) with a heating rate of 10 °C min<sup>-1</sup> under nitrogen.

### 2.3 Synthesis of poly(aryl ether ketone) polymer P

The 4,4-bis(4-hydroxyphenyl) pentanoic acid (3.58 g, 12.50 mmol), 2,2-bis(4-hydroxyphenyl) propane (2.85 g, 12.50 mmol), potassium carbonate (7.00 g, 36.23 mmol), 60 mL dimethyl sulfoxide and 30 mL toluene were added to the flask. The mixture was refluxed at 120 °C under nitrogen for 2 h. After the toluene was distilled, the

4,4-difluoro-benzophenone (5.45 g, 25.00 mmol) was added and the temperature was increased to 170 °C and held there for 10 h. Next, the sample was cooled to ambient temperature, and the mixture was divided into liquid and solid phases. After the liquid phase was removed, the solid was dissolved in 300 mL of a mixture of tetrahydrofuran and concentrated hydrochloric acid at a volume ratio of 3:1. The solution was then poured into 3000 mL amount of water and stirred for 20 h. The solid phase was then collected, milled into powder, washed with hot water and dried under vacuum at 50 °C for 96 h. The yield was 70%. The <sup>1</sup>H-NMR (CDCl<sub>3</sub>): δ = 1.96 (s, 9H), 2.13 (t, 2H), 2.39 (t, 2H), 7.11 (d, 16H), 7.30 (d, 8H), and 7.88 (t, 8H); FT-IR (KBr): 3200–3500 cm<sup>-1</sup> (–COOH), 1738 cm<sup>-1</sup> (–C=O), 1593, 1498 cm<sup>-1</sup> (–Ar–), 1242 and 1014 cm<sup>-1</sup> (Ar–O).

### 2.4 Synthesis of EO polymer P1

Polymer P (0.50 g), chromophore TCF-G (0.18 g, 0.50 mol) and 1,4-dimethylpyridinium *p*-toluenesulfonate (0.06 g, 0.06 mol) were dissolved in 30 mL mixture of tetrahydrofuran/dichloromethane (1:1). The mixture was stirred under nitrogen for 15 min, and *N,N*-dicyclohexyl carbodiimide (0.13 g, 0.65 mol) was added. The mixture was then stirred at ambient temperature for one night. The solid residue was filtered when the reaction was completed. The filtrate was precipitated in methanol to afford a purple solid. This solid was dried under vacuum at 50 °C for 96 h with 36% yield. <sup>1</sup>H-NMR (CDCl<sub>3</sub>): δ = 1.43(s, 0.9H), 1.96 (s, 9H), 2.13 (t, 2H), 2.39 (t, 2H), 3.23(s, 0.45H), 3.87(s, 0.3H), 4.39(s, 0.3H), 6.9–7.30 (m, 25H), and 7.88 (t, 8H); FT-IR(KBr): 3200–3500 cm<sup>-1</sup> (–COOH), 2225 cm<sup>-1</sup> (–C≡N), 1736 cm<sup>-1</sup> (–C=O), 1652 cm<sup>-1</sup> (–C=C–), 1593, 1498 cm<sup>-1</sup> (–Ar–), 1242, 1014 cm<sup>-1</sup> (Ar–O), 1161 cm<sup>-1</sup> [–C(=O)–O], and 1066 cm<sup>-1</sup> (–O–).

### 2.5 Synthesis of EO polymer P2

Polymer P (0.25 g), chromophore TCP-G (0.18 g, 0.50 mol) and 1,4-dimethylpyridinium *p*-toluenesulfonate (0.06 g, 0.06 mol) were dissolved in 30 mL mixture of tetrahydrofuran/dichloromethane (1:1). The mixture was stirred under nitrogen atmosphere for 15 min, and then *N,N*-dicyclohexyl carbodiimide (0.13 g, 0.65 mol) was added. Then the mixture was stirred at ambient temperature for one night. The solid residue was filtered when the reaction finished. The filtrate was precipitated in methanol to afford a green solid. The solid was dried under vacuum at 50 °C for 96 h with 33% yield. <sup>1</sup>H-NMR (CDCl<sub>3</sub>): δ = 0.9–1.1(m, 3.4H), 1.43(s, 0.9H), 1.96 (s, 9H), 2.13 (t, 2H), 2.39 (t, 2H), 3.23(s, 0.3H), 3.87(s, 0.2H), 4.39(s, 0.3H), 6.9–7.30 (m, 25H), and 7.88 (t, 8H); FT-IR(KBr): 3200–3500 cm<sup>-1</sup> (–COOH), 2225 cm<sup>-1</sup>

( $-\text{C}\equiv\text{N}$ ),  $1734\text{ cm}^{-1}$  ( $-\text{C}=\text{O}$ ),  $1651\text{ cm}^{-1}$  ( $-\text{C}=\text{C}-$ ),  $1608$ ,  $1485\text{ cm}^{-1}$  ( $-\text{Ar}-$ ),  $1242$ ,  $1037\text{ cm}^{-1}$  ( $\text{Ar}-\text{O}$ ),  $1136\text{ cm}^{-1}$  [ $-\text{C}(=\text{O})-\text{O}$ ], and  $1066\text{ cm}^{-1}$  ( $-\text{O}-$ ).

## 2.6 Preparation of the EO films

The 0.2 g of **P1** or **P2** was dissolved in 1.0 mL cyclopentanone and stirred for 5 h. The mixture was then filtered with a  $0.2\text{ }\mu\text{m}$  filter. The solution was spin-coated on indium tin oxides glass at  $500\text{--}600\text{ r min}^{-1}$ , and the films were then dried under vacuum at  $40\text{ }^\circ\text{C}$  for 24 h. The thickness of the films was varied from 2 to  $4\text{ }\mu\text{m}$ .

## 2.7 Structure characterization of polymer P1 and P2

The structure of polymers **P1** and **P2** were characterized by FTIR,  $^1\text{H-NMR}$  and UV–Vis spectroscopy. Three characteristic peaks were picked out for the polymer before post-functionalization: (1) the strong vibration absorption peak at  $1242\text{ cm}^{-1}$  confirmed the structure's aromaticity; (2) the absorption peak at  $1738\text{ cm}^{-1}$  confirms the ketone carbonyl; and (3) the wide absorption peak between  $3200$  and  $3500\text{ cm}^{-1}$  indicates a carboxyl groups. After post functionalization, polymers **P1** and **P2** show three other characteristic peaks:  $1066\text{ cm}^{-1}$  for  $\text{C}-\text{O}-\text{C}$ ;  $1625\text{ cm}^{-1}$  for  $-\text{C}=\text{C}-$ ; and  $2225\text{ cm}^{-1}$  for  $-\text{C}\equiv\text{N}$ .

The weight-average molecular weights ( $M_w$ ) of **P**, **P1** and **P2** are shown in Table 1. The weight-average molecular weights of EO polymer **P1** and **P2** are smaller than polymer **P**. The polydispersity ( $M_w/M_n$ ) of EO polymers **P1** and **P2** increase according to polymer **P**. These results indicate that some of the polymer chain segments of polymer **P** are broken during the synthesis. The weight-average molecular weights for **P1** and **P2** are around  $10^4$ , which is suitable for use as EO materials due to their solubility and machinability.

## 2.8 Solubility of polymer P1 and P2

Next, we measured the solubility of polymers **P1** and **P2**. Both showed good solubility in normal solvents such as *N,N*-dimethylformamide, acetone, tetrahydrofuran and chloroform. The 30–35 wt% polymers **P1** and **P2** could be solvated, and these were enough for use in polymer EO device preparation. This solubility is attributed to their large side chains, which could restrain the regular arrangement of the principal chain and reduce the corresponding interactions. In contrast, the films prepared in 1,1-dichloroethane from polymer **P1** and **P2** are very smooth with no phase separation. These results confirmed that such polymers could be used in the preparation of optical films.

## 2.9 Linear optical character of polymer P1 and P2

Table 1 presents UV–Vis absorption data for **P1** and **P2** in dichloromethane solution and films. Polymer **P2** shows a larger  $\lambda_{\text{max}}$  in both dichloromethane solution and film. This result confirms that the energy gap between the highest occupied molecular orbital (HOMO) and lowest unoccupied molecular orbital (LUMO) for chromophore **TCP-G** was lower than in chromophore **TCF-G**. The lower energy gap is usually related to higher intra-molecular mobility of the electron cloud for corresponding chromophores. Chromophore **TCP-G** shows better microscopic electro-optic hyperpolarizability.

## 2.10 Thermal characteristics of P1 and P2

The TGA curves for polymers **P**, **P1** and **P2** are shown in Fig. 2. The weight loss of **P**, **P1** and **P2** could be divided into two temperature sections. Between  $135$  and  $160\text{ }^\circ\text{C}$ , the carboxyl groups were reduced affording anhydride groups. This improved the thermal stability. The **P**, **P1** and **P2** polymers

**Table 1** Principal parameters of poled copolymers

Polymer	$M_w^a (\times 10^4)$	$M_w/M_n$	$\lambda_{\text{max}}$ (nm)		$T_g^d$ ( $^\circ\text{C}$ )	$T_d^e$ ( $^\circ\text{C}$ )	Chromophore content (wt%)	$r_{33}$ (pm/V) <sup>f</sup>	$r_{33}$ (pm/V) <sup>g</sup>
			Solution <sup>b</sup>	Film <sup>c</sup>					
<b>P</b>	2.85	2.58	–	–	158	398	–	–	–
<b>P1</b>	2.39	4.12	571	574	165	315	18	19.3	6.7
<b>P2</b>	2.46	4.06	702	698	151	350	23	46.5	26

<sup>a</sup>Measured by GPC in THF on the basis of a polystyrene calibration

<sup>b</sup> $\lambda_{\text{max}}$  of polymer solutions in  $\text{CH}_2\text{Cl}_2$

<sup>c</sup> $\lambda_{\text{max}}$  of spin-coated films

<sup>d</sup>Glass transition temperature, determined by DSC at a heating rate of  $10\text{ }^\circ\text{C min}^{-1}$  under nitrogen with a gas flow of  $50\text{ mL min}^{-1}$

<sup>e</sup>The 5% weight loss temperature as detected by the TGA analyses under nitrogen at a heating rate of  $10\text{ }^\circ\text{C min}^{-1}$

<sup>f</sup>Measured by a simple reflection technique at  $1310\text{ nm}$

<sup>g</sup>Chromophores doped in PC forming guest–host system [39, 44]

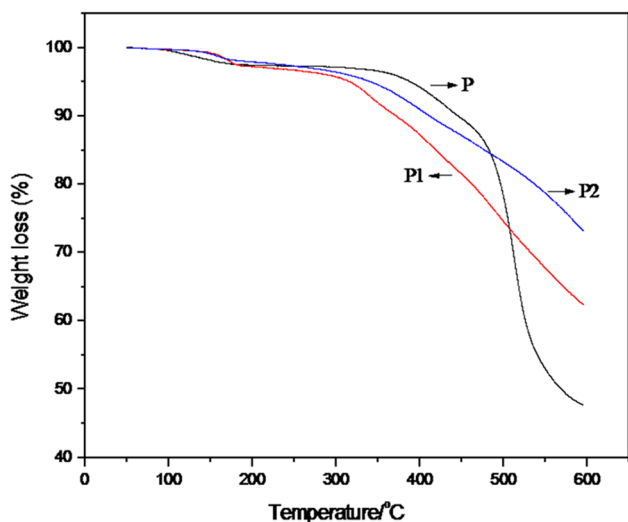


Fig. 2 Thermogravimetric analysis curves for **P**, **P1** and **P2** polymers

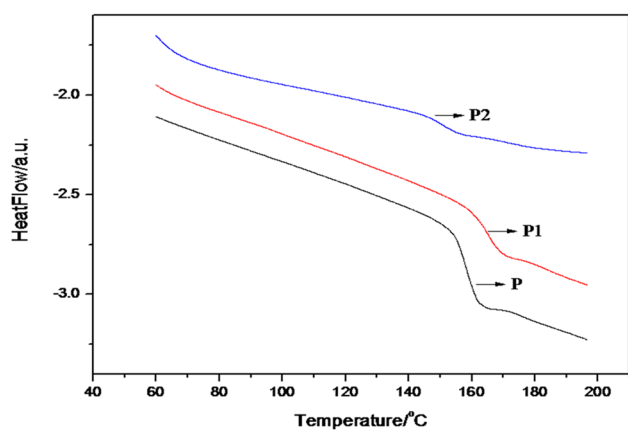


Fig. 3 Differential scanning calorimetry curves for polymers **P**, **P1** and **P2**

started to decompose at 398, 315 and 350 °C, respectively. The thermal decomposition temperatures were 280 and 308 °C for chromophore **TCF-G** and **TCP-G**, respectively [51, 52]. The thermal stability was improved by more than 30 °C compared to chromophore **TCF-G** and **TCP-G** after attaching the polymer. The high thermal decomposition temperature of these polymers was mainly determined by the special chemical stability of aryl ether ketone.

The differential scanning calorimetry (DSC) curves of polymers **P**, **P1** and **P2** are shown in Fig. 3. The glass transition temperatures for polymers **P1** and **P2** were much lower than their thermal decomposition temperature indicating that all of the polymers had an amorphous structure. Due to the specific structure of the polymer with a large amount of aromatic rings and carboxyl groups, polymer **P** demonstrates a higher glass transition temperature (158 °C).

The glass transition temperature of **P1** improved to 165 °C after introducing chromophore **TCF-G**, though the electrostatic interactions among the backbone of the polymer were reduced. The glass transition temperature increased because of dipole–dipole interactions among chromophore **TCF-G**, improvements in hydrogen bonding interactions, and the rigid structure of chromophore **TCF-G**.

The glass transition temperature of polymer **P2** was reduced to 151 °C after introduction of chromophore **TCP-G**. The reduction in the glass transition temperature for polymer **P2** was attributed to the larger modified group in chromophore **TCP-G** that reduces the dipole–dipole interactions among chromophores as well as minimized hydrogen bonding. Most EO devices are stable at below 100 °C. The glass transition temperature above 150 °C confirms the material’s stability in normal device working environments.

The regular structure of poly(aryl ether ketone) determined the interaction among the polymer chain segments. The strong interaction among the polymer chain segments confirmed the high glass transition temperature of the polymers. Such result had positive effects on improving the long term stability of organic EO polymers.

### 2.11 EO efficiency of polymers **P1** and **P2**

Poling is an important process that can align the chromophores. We performed alignment by corona poling under the following conditions: (1) the poling temperature was about 5 °C higher than the Tg of the EO polymer; (2) the poling voltage was about 8 kV; (3) the poling process lasted for 10 min. When the poling process finished, the sample was subsequently cooled to ambient temperature and then the applied voltage was switched off. The poling conditions should be optimized for every kind of EO polymer. During optimization, the poling process showed no damage of the films, and the higher EO coefficients were achieved and reported. The materials were not damaged with a poling voltage of about 8 kV.

After corona poling, the dipole moments of the chromophore moieties in the polymer were aligned, and the absorption curve decreased due to birefringence [38, 39]. From their absorption change, the order parameter ( $\Phi$ ) for polymer was calculated according to the following equation:

$$\Phi = 1 - A_1/A_0 \tag{2}$$

$A_1$  and  $A_0$  are the  $\lambda_{max}$  of the polymer film before and after corona poling, respectively. The UV–Vis spectra before and after poling process are shown in Fig. 4 (left) and 4 (right) for the polymers **P1** and **P2**, respectively. The calculated  $\Phi$  values are presented in Fig. 4 for **P1** and **P2** and were equal to 20 and 19%, respectively. This result indicated that the poling efficiency was higher than some other EO polymers; the  $\Phi$  values were about 14–17% [49, 50].

The EO efficiencies of poled films were determined by a simple reflection technique initially proposed by Teng and Man [40]. The  $r_{33}$  values were calculated using the following equation:

$$r_{33} = \frac{3\lambda I_m}{4\pi V_m I_c n^2} \frac{(n^2 - \sin^2\theta)^{3/2}}{(n^2 - 2\sin^2\theta)} \frac{1}{\sin^2\theta} \quad (3)$$

Here,  $r_{33}$  is the EO coefficient of the poled polymer,  $\lambda$  is the probing optical wavelength,  $\theta$  is the incident angle,  $I_c$  is the output beam intensity,  $I_m$  is the amplitude of the modulation,  $V_m$  is the modulating voltage, and  $n$  is the refractive index of the polymer films. The EO coefficient usually depends on the concentration of chromophore. The highest obtained  $r_{33}$  values were 19.3 and 46.5 pm/V, respectively, for EO polymers **P1** and **P2**, respectively at 1310 nm. The largest  $r_{33}$  values for chromophore TCF-G was equal to about 6.7 pm/V and the  $r_{33}$  values for chromophore TCP-G was 26 pm/V [39, 44]. For every kind of EO polymer, five samples should be prepared and poled after the optimization of poling conditions. The largest EO coefficients for every EO films are collected and their arithmetic means are determined as their EO coefficients.

To clarify the role of the particular chromophores, we performed additional quantum chemical simulations particularly for the second order hyperpolarizabilities at a wavelength of 1.3  $\mu\text{m}$ . It should be emphasized that the chromophore ground state dipole moments are critical in the EO effect. Chromophores were optimized using Gaussian W09 quantum chemical package [45, 46]. The initial geometries

of the molecules were estimated by the PM6 method, and then optimized using the DFT B3LYP method and the 6-31G basis set [47, 48]. The results show that **P1** has a higher dipole moment, but **P2** has a larger  $\beta$  magnitude (Table 2).

The calculated values of hyperpolarizabilities play more important roles in the prediction of EO efficiencies than dipole moments in the case of polymer amorphous compounds in which monomers are not linked together through electron bridges such as double bonds or aromatic systems. This is also true in our case: the EO coefficient of **P2** is higher than that for **P1** as well as the hyperpolarizability of **P2** is higher than **P1**.

For most of macromolecules, general dipole moment is not so crucial. Rather, the difference between charges of neighbored electron donors and acceptor parts are more important because huge substituents (such as **P2**) can significantly change the magnitude of the dipole moment without principal changes in the interaction character of neighboring electron donor and acceptor parts. For amorphous substances, a positively charged center can be involved in electrostatic interactions with negative ones from another part of the macromolecule or another molecule and *vice versa*.

**Table 2** Theoretically calculated ground state dipole moments and hyperpolarizabilities ( $\lambda = 1.3 \mu\text{m}$ ) for **P1** and **P2**

Dipole moment (D)		$\beta$ (esu)	
<b>P1</b>	<b>P2</b>	<b>P1</b>	<b>P2</b>
18.7773	13.3389	$1.2323\text{E}^{-29}$	$1.4653\text{E}^{-29}$

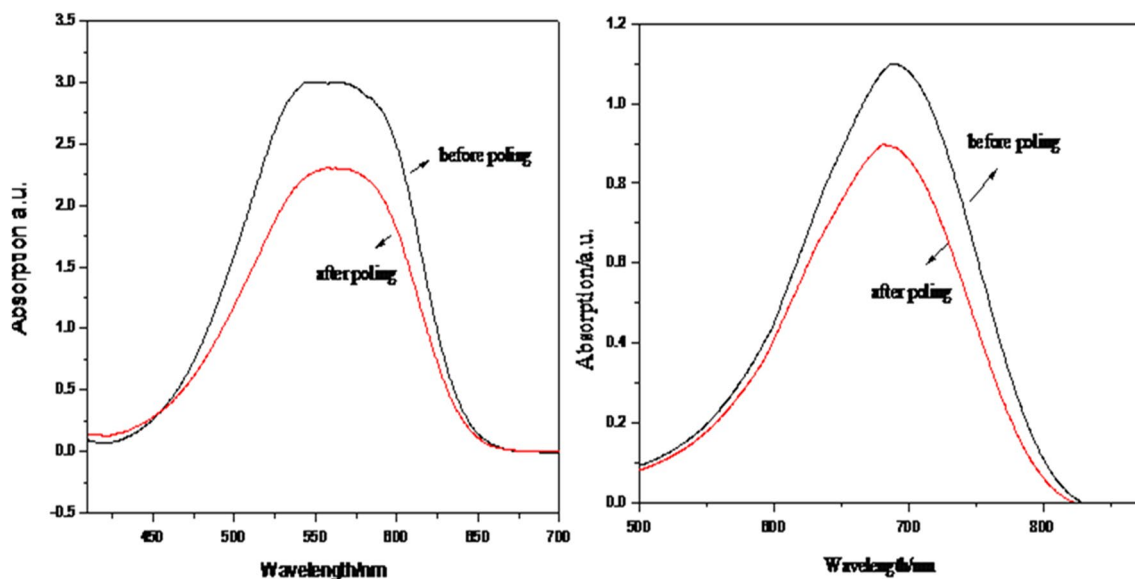


**Fig. 4** UV-Vis spectra for the titled EO polymers: **P1** (left) and **P2** (right)

Real polymers have many possible conformations and dipole moments.

### 2.12 Long-term stability of the crosslinking system

The long-term stability of the EO activity is an important property for device fabrication. In later fabrication, the poled EO polymer must resist temperatures up to 80 °C to complete the photolithography. To investigate the long-term NLO stability of the poled polymers, a normalized EO coefficient [ $r_{33}(t)/r_{33}(t_0)$ ] was measured as a function of time at 80 °C. Figure 5 shows that a fast decay was observed in the first 50 h for both **P1** and **P2**. This was due to the recovery of bond angles and bond lengths in the oriented chromophores. Next, the  $r_{33}$  values remained nearly constant in the remaining time. The initial  $r_{33}$  values held 80 and 88% of their values after 500 h of heating at 80 °C for **P1** and **P2**, respectively. If the recovery process of bond angles and bond lengths in the aligned chromophores was moved away, the  $r_{33}$  values at 50 h was settled as the initial values, the long term stability will be improved to another attitude. This will reach up to 93 and 99%, respectively for polymer **P1** and **P2**. Such long term stability was due to the high glass transition temperature of polymer **P1** and **P2**, which was determined by the special structure of ketones in the main chain of these polymers.

In theory, the chromophore in polymer **P2** has a larger inter-spatial volume, and polymer **P2** should have worse long-term stability [43, 55]. However, Fig. 5 showed opposite results. The structures of **P1** and **P2** shown in Fig. 1 show that **P2** is surrounded by more flexible chains, and the dipole interaction among the chromophore molecules was reduced greatly. Thus, the induced interaction was the main factor influencing the long-term stability of EO polymer. This was greatly reduced, and polymer **P2** demonstrated long-term stability.

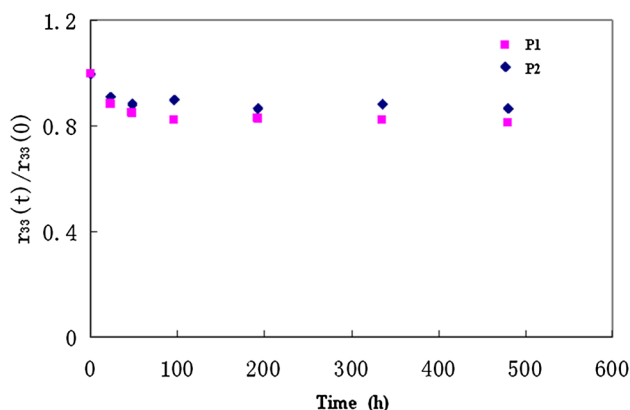


**Fig. 5** Long-term stability of EO polymers **P1** and **P2**

## 3 Conclusions

A novel poly(aryl ether ketone) polymer **P** with a high glass transition temperature was synthesized based on the monomers of 4,4-bis(4-hydroxyphenyl) pentanoic acid, 2,2-bis(4-hydroxyphenyl) propane and 4,4-difluoro-benzophenone. The organic non-linear optical chromophore TCF-G and TCP-G were attached to polymer **P**, and afforded us two excellent EO polymers: **P1** and **P2**. These products have good solubility in common solvents, and their high glass transition temperatures confirmed their machinability and stability. The EO films prepared from **P1** and **P2** had higher EO coefficients (46.5 pm/V) than the host–guest doping system (26 pm/V) [44]. Due to the high glass transition temperatures and poor dipole interactions among the chromophores, these EO polymers have excellent long-term stabilities. Even after heating at 80 °C for 500 h, 89% of the EO activity remains. This was confirmed with additional quantum chemical simulations of the principal molecular fragments. These simulations have shown that the hyperpolarizabilities play more important role in the prediction of EO efficiencies than the ground state dipole moments. This is true for the case of polymer amorphous compounds in which monomers are not linked together through electron bridges including double bonds or aromatic systems.

**Acknowledgements** We are grateful to the National Natural Science Foundation of China (No. 51503215) and the Fund of Key Laboratory of Agrifood Safety and Quality, MOA (2016-KF-14) for financial support. Also, the authors are grateful to the Deanship of Scientific Research, King Saud University for funding through Vice Deanship of Scientific Research Chairs.

### Compliance with ethical standards

**Conflict of interest** The authors declare no conflict of interest.

**Open Access** This article is distributed under the terms of the Creative Commons Attribution 4.0 International License (<http://creativecommons.org/licenses/by/4.0/>), which permits unrestricted use, distribution, and reproduction in any medium, provided you give appropriate credit to the original author(s) and the source, provide a link to the Creative Commons license, and indicate if changes were made.

## References

1. W. Gao, G. Qin, J. Liu, Design and preparation of novel Diels–Alder crosslinking polymer and its application in NLO materials. *J. Mater. Sci.* **28**, 8480–8486 (2017)
2. S. Benight, D. Bale, B. Olbricht, L. Dalton, Organic electro-optics: understanding material structure/function relationships and device fabrication issues. *J. Mater. Chem.* **19**, 7466–7475 (2009)
3. J. Liu, G. Xu, F. Liu, I. Kityk, X. Liu, Z. Zhen, Recent advances in polymer electro-optic modulators. *RSC Adv.* **5**, 15784 (2015)



- A. Yin, Q. He, Z. Lin, L. Luo, Y. Liu, S. Yang, H. Wu, M. Ding, Y. Huang, X. Duan, Plasmonic/nonlinear optical material core/shell nanorods as nanoscale plasmon modulators and optical voltage sensors. *Angew. Chem. Int. Edit* **55**, 583–587 (2016)
- V. Katopodis, P. Groumas, Z. Zhang, R. Dinu, E. Miller, A. Konczykowska, J.Y. Dupuy, A. Beretta, A. Dede, J.H. Choi, Polymer enabled 100 Gbaud connectivity for datacom applications. *Opt. Commun.* **362**, 13–21 (2016)
- F. Qiu, H. Sato, A.M. Spring, D. Maeda, M. Ozawa, K. Odoi, I. Aoki, A. Otomo, S. Yokoyama, Ultra-thin silicon/electro-optic polymer hybrid waveguide modulators. *Appl. Phys. Lett.* **107**, 123302 (2015)
- Y. Enami, Y. Jouane, J. Luo, A.K.Y. Jen, Enhanced conductivity of sol-gel silica cladding for efficient poling in electro-optic polymer/TiO<sub>2</sub> vertical slot waveguide modulators. *Opt. Express* **22**, 30191–30199 (2014)
- J. Liu, W. Gao, I. Kityk, X. Liu, Z. Zhen, Optimization of polycyclic electron-donors based on julolidinyl structure in push-pull chromophores for second order NLO effects. *Dyes Pigment* **122**, 74–84 (2015)
- J. Liu, P. Si, X. Liu, Z. Zhen, Copper-catalyzed Huisgen cycloaddition reactions used to incorporate NLO chromophores into high T<sub>g</sub> side-chain polymers for electro-optics. *Opt. Mater.* **47**, 256–262 (2015)
- J. Liu, W. Gao, X. Liu, Z. Zhen, Benefits of the use of auxiliary donors in the design and preparation of NLO chromophores. *Mater. Lett.* **143**, 333–335 (2015)
- Y. Jouane, Y. Chang, D. Zhang, J. Luo, A.K.Y. Jen, Unprecedented highest electro-optic coefficient of 226 pm/V for electro-optic polymer/TiO<sub>2</sub> multilayer slot waveguide modulators. *Opt. Express* **22**, 27725–27732 (2014)
- Y.C. Chen, T.Y. Juang, T.M. Wu, S.A. Dai, W.J. Kuo, Y.L. Liu, F. Chen, R.J. Jeng, Orderly arranged NLO materials on exfoliated layered templates based on dendrons with alternating moieties at the periphery. *Polym. Chem.* **4**, 2747–2759 (2013)
- S. Farsadpour, L. Ghoochany, C. Kaiser, G. Von Freymann, New class of hyperpolarizable push-pull organic chromophores by applying a novel and convenient synthetic strategy. *Dyes Pigment* **127**, 73–77 (2016)
- B. Coe, D. Rusanova, V. Joshi, S. Sánchez, J. Vávra, D. Khobragade, L. Severa, I. Císařová, D. Šaman, R. Pohl, K. Clays, G. Depotter, B. Brunschwig, F. Teplý, Helquat dyes: helicene-like push-pull systems with large second-order nonlinear optical responses. *J. Org. Chem.* **81**, 1912–1920 (2016)
- H. Wang, M. Zhang, Y. Yang, F. Liu, C. Hu, H. Xiao, L. Qiu, X. Liu, J. Liu, Z. Zhen, Synthesis and characterization of one novel second-order nonlinear optical chromophore based on new benzoxazin donor. *Mater. Lett.* **164**, 644–646 (2016)
- F. Bureš, D. Cvejn, K. Melánová, L. Beneš, J. Svoboda, V. Zima, O. Pytela, T. Mikysek, Z. Růžicková, I. Kityk, A. Wojciechowski, N. AlZayed, Effect of intercalation and chromophore arrangement on the linear and nonlinear optical properties of model aminopyridine push-pull molecules. *J. Mater. Chem. C* **4**, 468–478 (2016)
- Y. Yang, S. Bo, H. Wang, F. Liu, J. Liu, L. Qiu, Z. Zhen, X. Liu, Novel chromophores with excellent electro-optic activity based on double-donor chromophores by optimizing thiophene bridges. *Dyes Pigment* **122**, 139–146 (2015)
- Y. Shi, D. Frattarelli, N. Watanabe, A. Facchetti, E. Cariati, S. Righetto, E. Tordin, C. Zuccaccia, A. Macchioni, S. Wegener, C. Stern, M. Ratner, T. Marks, Ultra-high-response, multiply twisted electro-optic chromophores: influence of pi-system elongation and interplanar torsion on hyperpolarizability. *J. Am. Chem. Soc.* **137**, 12521–12538 (2015)
- J. Liu, Y. Yang, X. Liu, Z. Zhen, Physical attachment of NLO chromophores to polymers for great improvement of long-term stability. *Mater. Lett.* **142**, 87–89 (2015)
- G. Deng, H. Huang, P. Si, H. Xu, J. Liu, S. Bo, X. Liu, Z. Zhen, L. Qiu, Synthesis and electro-optic activities of novel polycarbonates bearing tricyanopyrroline-based nonlinear optical chromophores with excellent thermal stability of dipole alignment. *Polymer* **54**, 6349–6356 (2013)
- D. Deng, S. Bo, T. Zhou, H. Huang, J. Wu, J. Liu, X. Liu, Z. Zhen, L. Qiu, Facile synthesis and electro-optic activities of new polycarbonates containing tricyanofuran-based nonlinear optical chromophores. *J. Polym. Sci. Pol. Chem.* **51**, 2841–2849 (2013)
- J. Liu, L. Wang, Z. Zhen, X. Liu, Synthesis of novel polyarylate with electrooptical chromophores as side chain as electro-optic host polymer. *Colloid Polym. Sci.* **290**, 1215–1220 (2012)
- Y. Mori, K. Nakaya, X. Piao, K. Yamamoto, A. Otomo, S. Yokoyama, Large electro-optic activity and enhanced temporal stability of methacrylate-based crosslinking hyperbranched nonlinear optical polymer. *J. Polym. Sci. Pol. Chem.* **50**, 1254–1260 (2012)
- F. Borbone, A. Carella, A. Roviello, M. Casalboni, F. De Matteis, G. Stracci, F. della Rovere, A. Evangelisti, M. Dispenza, Outstanding poling stability of a new cross-linked nonlinear optical (NLO) material from a low molecular weight chromophore. *J. Phys. Chem. B* **115**, 11993–12000 (2011)
- R. Zhang, J. Liu, S. Bo, G. Deng, C. Peng, X. Liu, Z. Zhen, Synthesis and electro-optical features of a high T<sub>g</sub> polymer system with excellent electro-optic activity and thermal stability. *Colloid Polym. Sci.* **290**, 1819–1823 (2012)
- F. Yu, A.M. Spring, L. Li, F. Qiu, K. Yamamoto, D. Maeda, M. Ozawa, K. Odoi, S. Yokoyama, An enhanced host-guest electro-optical polymer system using poly(norbornene-dicarboximides) via ROMP. *J. Polym. Sci. Pol. Chem.* **51**, 1278–1284 (2013)
- W. Huang, Z. Jin, Z. Shi, J.J. Intemann, M. Li, J. Luo, A.K.Y. Jen, Spontaneous thermal crosslinking of a sydnone-containing side-chain polymer with maleimides through a convergent [3 + 2] dual cycloaddition/cycloreversion process for electro-optics. *Polym. Chem.* **4**, 5760–5767 (2013)
- J. Liu, H. Xu, X. Liu, Z. Zhen, W. Kuznik, I.V. Kityk, Novel promising crosslinkable tricyanopyrroline polymeric electro-optic materials. *J. Mater. Sci. Mater. Electron* **23**, 1182–1187 (2012)
- Z. Shi, J. Luo, S. Huang, B.M. Polishak, X.H. Zhou, S. Liff, T.R. Younkin, B.A. Block, A.K.Y. Jen, Achieving excellent electro-optic activity and thermal stability in poled polymers through an expeditious crosslinking process. *J. Mater. Chem.* **22**, 951–959 (2012)
- Z. Shi, S. Hau, J. Luo, T.D. Kim, N.M. Tucker, J.W. Ka, H. Sun, A. Pyajt, L. Dalton, A. Chen, A.K.Y. Jen, Highly efficient diels-alder crosslinkable electro-optic dendrimers for electric-field sensors. *Adv. Funct. Mater.* **17**, 2557–2563 (2007)
- G.N. Nazmieva, T.A. Vakhonina, N.V. Ivanova, A.S. Mukhtarov, N.N. Smirnov, A.V. Yakimansky, M.Y. Balakina, O.G. Sinyashin, Testing of the ways for synthesis of new nonlinear optical epoxy-based polymers with azochromophores in the side chain. *Eur. Polym. J.* **63**, 207–216 (2015)
- T.A. Vakhonina, M.Y. Balakina, G.N. Nazmieva, N.V. Ivanova, S.V. Kurmaz, I.S. Kochneva, M.L. Bubnova, E.O. Perepelitsina, N.N. Smirnov, A.V. Yakimansky, O.G. Sinyashin, Synthesis and nonlinear optical properties of branched copolymers with covalently attached azochromophores. *Eur. Polym. J.* **50**, 158–167 (2014)
- C. Peng, J. Wu, J. Liu, L. Qiu, X. Liu, S. Bo, Z. Zhen, Synthesis and optical properties of new fluorinated second-order nonlinear optical copolymers: an attempt toward the balance between solubility and long-term alignment stability. *Polym. Chem.* **4**, 2703–2708 (2013)
- Z. Li, J. Hua, Q. Li, C. Huang, A. Qin, C. Ye, J. Qin, Synthesis of novel poly {methyl-[3-(9-indolyl)propyl]siloxane}-based nonlinear optical polymers via postfunctionalization. *Polymer* **46**, 11940–11948 (2005)

35. Q. Zeng, G. Qiu, C. Ye, J. Qin, Z. Li, New second-order nonlinear optical polyphosphazenes: convenient postfunctionalization synthetic approach and application of the concept of suitable isolation group. *Dyes Pigment* **84**, 229–236 (2010)
36. R. Tang, H. Chen, S. Zhou, B. Liu, D. Gao, H. Zeng, Z. Li, The integration of an “X” type dendron into polymers to further improve the comprehensive NLO performance. *Polym. Chem.* **6**, 5580–5589 (2015)
37. W. Wu, R. Xiao, W. Xiang, Z. Wang, Z. Li, Main chain dendronized polymers: design, synthesis, and application in the second-order nonlinear optical (NLO) area. *J. Phys. Chem. C* **119**, 14281–14287 (2015)
38. J. Liu, W. Hou, S. Feng, L. Qiu, X. Liu, Z. Zhen, Synthesis and nonlinear optical properties of branched pyrroline chromophores. *J. Phys. Org. Chem.* **24**, 439–444 (2011)
39. J. Liu, S. Bo, X. Liu, Z. Zhen, Enhanced poling efficiency in rigid-flexible dendritic nonlinear optical chromophores. *J. Incl. Phenom. Macrocycl. Chem.* **68**, 253–260 (2010)
40. C. Teng, H. Man, Simple reflection technique for measure the electrooptic coefficient of poled polymers. *Appl. Phys. Lett.* **56**, 1734–1736 (1990)
41. F. Bureš, H. Čermáková, J. Kulhánek, M. Ludwig, M. Kuznik, I.V. Kityk, T. Mikysek, A. Růžička, Structure-property relationships and nonlinear optical effects in donor-substituted dicyanopyrazine-derived push-pull chromophores with enlarged and varied pi-linkers. *Eur. J. Org. Chem.* **2012**, 529–538 (2012)
42. J. Kulhánek, F. Bureš, W. Kuznik, I.V. Kityk, T. Mikysek, A. Růžička, Ferrocene-donor and 4,5-dicyanoimidazole-acceptor moieties in charge-transfer chromophores with p linkers tailored for second-order nonlinear optics. *Chem. Asian J.* **8**, 465–475 (2013)
43. J. Liu, H. Huang, X. Liu, Z. Zhen, Synthesis of nonlinear optical chromophore and the preparation of attenuated total reflectance modulator. *Polym. Adv. Technol.* **23**, 866–869 (2012)
44. W. Zhao, Z. Wang, Z. Chen, G. Xu, X. Han, L. Qiu, Z. Zhen, X. Liu, Synthesis and properties of a novel cross linked poled polymer. *Photogr. Sci. Photochem.* **25**, 452–459 (2007)
45. M. Frisch, G.W. Trucks, H.B. Schlegel, G.E. Scuseria, M.A. Robb, J.R. Cheeseman, G. Scalmani, V. Barone, B. Mennucci, G.A. Petersson, H. Nakatsuji, M. Caricato, X. Li, H. Hratchian, A.F. Izmaylov, J. Bloino, G. Zheng, J.L. Sonnenberg, M. Hada, M. Ehara, K. Toyota, R. Fukuda, L. Hasegawa, M. Ishida, N. Nakajima, Y. Honda, O. Kitao, H. Nakai, T. Vreven, J.A. Montgomery, J.E. Peralta, F. Ogliaro, M. Bearpark, J.J. Heyd, E. Brothers, K.N. Kudin, V.N. Staroverov, R. Kobayashi, J. Normand, K. Raghavachari, A. Rendell, J.C. Burant, S.S. Iyengar, J. Tomasi, M. Cossi, N.M. Rega, J.M. Millam, M. Klene, J.E. Knox, J.B. Cross, V. Bakken, J. Adamo, C.Jaramillo, R. Gomperts, R.E. Stratmann, O. Yazyev, A.J. Austin, R. Cammi, C. Pomelli, J.W. Ochterski, R.L. Martin, K. Morokuma, V.G. Zakrzewski, G.A. Voth, P. Salvador, J.J. Dannenberg, S. Dapprich, A.D. Daniels, Ö Farkas, J.B. Foresman, J.V. Ortiz, J. Cioslowski, D.J. Fox, *Gaussian 09, revision C.01*. (Gaussian, Inc., Wallingford, 2009)
46. R. Dennington, T. Keith, J. Millam, *GaussView, version 5* (SemiChemInc., Shawnee Mission KS, 2009)
47. A.D. Becke, Density-functional exchange-energy approximation with correct asymptotic behavior. *Phys. Rev. A* **38**, 3098–3100 (1988)
48. C. Lee, W. Yang, R.G. Parr, Development of the Colle-Salvetti correlation-energy formula into a functional of the electron density. *Phys. Rev. B* **37**, 785–789 (1988)
49. J. Hao, M.J. Han, K. Guo, J. Zhai, T. Zhang, X. Meng, J. Liang, L. Qiu, Y. Shen, Synthesis and characterization of a cross-linkable nonlinear optical polymer functionalized with a thiophene and tricyanovinyl containing chromophore. *React. Funct. Polym.* **67**, 758–768 (2007)
50. Z. Li, S. Dong, P. Li, Z. Li, C. Ye, J. Qin, New PVK-based nonlinear optical polymers: enhanced nonlinearity and improved transparency. *J. Polym. Sci. A* **46**, 2983–2993 (2008)
51. W. Gao, J.L. Liu, Z. Chen, W.J. Hou, S.H. Bao, X.H. Liu, Z. Zhen, Synthesis of branched aniline-pyrroline chromophores and the research on their electro-optical properties. *Acta Chim. Sin.* **69**, 1225–1231 (2011)
52. W. Zhao, Z. Wang, Z. Chen, G. Xu, X. Han, L. Qiu, Z. Zhen, X. Liu, Synthesis and properties of a novel cross-linked poled polymer. *Photogr. Sci. Photochem.* **25**, 452–458 (2007)
53. X.H. Zhou, J. Davies, S. Huang, J. Luo, Z. Shi, B. Polishak, Y.J. Cheng, T.D. Kim, L. Johnson, A.K.Y. Jen, Facile structure and property tuning through alteration of ring structures in conformationally locked phenyltetraene nonlinear optical chromophores. *J. Mater. Chem.* **21**, 4437 (2011)
54. Y. Liao, B.E. Eichinger, K.A. Firestone, M. Haller, J. Luo, W. Kaminsky, J.B. Benedict, P.J. Reid, A.K.Y. Jen, L.R. Dalton, B.H. Robinson, Systematic study of the structure-property relationship of a series of ferrocenyl nonlinear optical chromophores. *J. Am. Chem. Soc.* **127**, 2758 (2005)
55. N. Tsutsumi, S. Yoshizaki, W. Sakai, T. Kiyotsukuri, Nonlinear optical polymers. I. Novel network polyurethane with azobenzene dye in the main frame. *Macromolecules* **28**, 6437–6442 (1995)
56. Y. Enami, H. Nakamura, J. Luo, A.K.Y. Jen, Analysis of efficiently poled electro-optic polymer/TiO<sub>2</sub> vertical slot waveguide modulators. *Opt. Commun.* **362**, 77–80 (2016)
57. S. Huang, J. Luo, H.L. Yip, A. Ayazi, X.H. Zhou, M. Gould, A. Chen, T. Baehr-Jones, M. Hochberg, A.K.Y. Jen, Efficient poling of electro-optic polymers in thin films and silicon slot waveguides by detachable pyroelectric crystals. *Adv. Mater.* **24**, OP42–OP47 (2012)
58. C. Koos, J. Leuthold, W. Freude, M. Kohl, L. Dalton, W. Bogaerts, A.L. Giesecke, M. Laueremann, A. Melikyan, S. Koeber, S. Wolf, C. Weimann, S. Muehlbrandt, K. Koehnle, J. Pfeifle, W. Hartmann, Y. Kutuvantavida, S. Ummethala, R. Palmer, D. Korn, L. Alloatti, P.C. Schindler, L. Delwin, D.L. Elder, T. Wahlbrink, J. Bolten, Silicon-organic hybrid (SOH) and plasmonic-organic hybrid (POH) integration. *J. Lightwave Technol.* **34**, 256–268 (2016)
59. A.M. Spring, F. Qiu, S. Yokoyama, High stability poly (*N*-adamantyl-exo-norbornene-5,6-dicarboximide) and phenyl vinylene thiophene electro-optic host-guest system. *Eur. Polym. J.* **84**, 89–99 (2016)
60. X. Zhang, C.J. Chung, A. Hosseini, H. Subbaraman, J. Luo, A.K.Y. Jen, R.L. Nelson, C. Lee, R.T. Chen, High performance optical modulator based on electro-optic polymer filled silicon slot photonic crystal waveguide. *J. Lightwave Technol.* **34**, 2941–2951 (2016)